RSC Advances

This article can be cited before page numbers have been issued, to do this please use: Y. ZHANG, C. Lim, W. Cai, R. Rohan, G. XU, Y. SUN and H. Cheng, *RSC Adv.*, 2014, DOI: 10.1039/C4RA08709G.

ROYAL SOCIETY OF CHEMISTRY

www.rsc.org/advances

View Article Online
DOI: 10.1039/C4RA08709G

Design and synthesis of a single ion conducting block copolymer electrolyte with multifunctionality for lithium ion batteries

Yunfeng Zhang,[a,b] Corina Anrou Lim,[a] Weiwei Cai,[a] Rupesh Rohan,[a] Guodong Xu,[a] Yubao Sun,[b] and Hansong Cheng[a,b*]

[a]Department of Chemistry, National University of Singapore, 3 Science Drive 3, Singapore, 117543

[b]Sustainable Energy Laboratory, China University of Geosciences Wuhan, 388 Lumo RD, Wuhan, 430074, China

E-mail: chghs2@gmail.com

Abstract

A novel single ion conducting block copolymer electrolyte (SI-co-PE) for applications in lithium-ion batteries is presented. The block copolymer is made of alternative ethylene oxide (EO) and aromatic segments to tune the glass transition temperature (T_g), the mechanical strength and the porosity of the material for achieving high electrochemical performance of lithium-ion batteries. Upon blending with a PVDF-HFP binder via a solution cast method, a gel SI-co-PE membrane with high ionic conductivity, a wide electrochemical window and a high lithium transference number was obtained. Excellent electrochemical stability and battery performance at both room temperature and 80 ^{o}C with various charge/discharge rates were demonstrated. The study underscores the fundamental importance of polymer electrolyte microstructures in battery performance enhancement and suggests ways to

View Article Online
DOI: 10.1039/C4RA08709G

improve the design of new electrolyte materials for development of better battery devices with a long cycle life.

Keywords: lithium ion battery, gel single ion conducting polymer electrolyte, block copolymer, battery performance.

1. Introduction

Gel polymer electrolytes (GPEs) containing liquid dual-ion inorganic lithium salts in low T_g flexible polymer matrices have made remarkable advances in the last decade and have been widely used in a variety of commercial applications, most notably in portable electronic devices.[1-8] GPEs exhibit many advantages over solid polymer electrolytes (SPEs) with better compatibility with electrodes in the charge-discharge cycling processes and substantially higher ion conductivity because of the introduction of organic solvents into polymer matrices, which reduce interfacial resistance and facilitate ion transport. Compared with liquid electrolytes, GPEs usually display a wider electrochemical window and high thermal stability.[9] Nevertheless, there still remain several key issues that need to be resolved for the GPE materials to compete with the conventional liquid electrolytes to achieve even broader applicability while maintaining substantially improved safety.[10] First, a high lithium ion transfer number close to unity would significantly raise the coulomb efficiency of battery devices.[11,12] Second, solution retention capacity must be enhanced for stable device performance. In principle, a high ionic conductivity requires a high carrier concentration.[13] For a GPE with a dual-ion lithium salt in a polymer matrix to achieve high ion conductivity, appropriate porosity including the

View Article Online
DOI: 10.1039/C4RA08709G

pore size, the volume fraction and the interconnectivity of pore domains in the polymer membrane is required to accommodate a large number of charge carriers.[14,15] In practice, a porous membrane with an average pore size of more than 1 μm usually causes an electrolyte leakage, leading to a deteriation of solution retention capacity, a degradation of ionic conductivity and a compromise of device safety.[16] Indeed, it has been a formidable challenge to obtain a GPE with both a high ionic conductivity and a strong mechanical strength because a membrane with high porosity weakens its mechanical strength.[17] Furthurmore, a strong concentration gradiant inherent to dual-ion based electrolytes during battery operation leads to dendrite growth and a low lithium ion tranference number (<0.3), which ultimately limits power delivery.[18,19]

Gel single ion conducting polymer electrolytes (Gel-SIPEs) have been found to offer an effective solution to the concentration gradiant problem with a high lithium ion transference number close to unity.[20-22] Several studies have demonstrated that lithium ion batteries assembled with gel-SIPE membranes display excellent electrochemical stability and device performance.[23-28] In this paper, we report design and synthesis of a gel single ion conducting block copolymer electrolyte (Gel-SI-co-PE) with a structure shown in Figure 1. The Gel-SI-co-PE membranes were fabricated using PVDF-HFP as a binder. All the membranes display high ion transference numbers close to unity. Three essential properties, i.e. ion conductivity, solution retention capacity and mechanical strength, were optimized simultaneously through tuning the ratio of the aliphatic and the aromatic segments of the polymers to

View Article Online
DOI: 10.1039/C4RA08709G

achieve high battery performance.[29] The two chemically dissimilar polymers, labelled as PEEIA and LiPEEPSI in Figure 1, are polymerized to form a block copolymer covalently bonded end-to-end. This architecture gives rise to local segregation or "microphase separation", resulting in formation of microporous domains to absorb a sufficient amount of solvent and to effectively prevent solution leakage from occuring with a pore diameter of less than 1 μm[30] as well as construction of continuous ion conducting channels upon formation of micropores.[31] Finally, the charge delocalized diphenylsulfonimide (DPSI) anions[32] were impregnated to the block copolymer backbone to minimize the concentration polarization effect upon charge/discharge usually observed in dual-ion based electrolytes. Lithium ions are thus attached to the immobilized polyanions through a weak electrostatic interaction with high mobility.[33-39] The membrane of the SI-co-PE complex was fabricated with a PVDF-HFP binder via a solution cast method and the thickness and flexibility of the resulting film were entirely tuneable. The membrane displays a low glass transition temperature as well as a high melting temperature. A macroporous morphology with an average pore size of ca. 200 nm and excellent mechanical strength of 27 MPa tensile stress was obtained. In addition, the membrane exhibits high electrochemical stability up to 4.3 V of oxidation voltage, high ionic conductivity of 3.9×10^{-4} S cm^{-1} at 25 ^{o}C and 1.2×10^{-3} S cm^{-1} at 80 ^{o}C and a high lithium ion transference number close to unity. Finally, excellent cyclic performance of the lithium battery assembled with the SI-co-PE based membrane at both an ambient temperature and an elevated temperature was demonstrated.

View Article Online
DOI: 10.1039/C4RA08709G

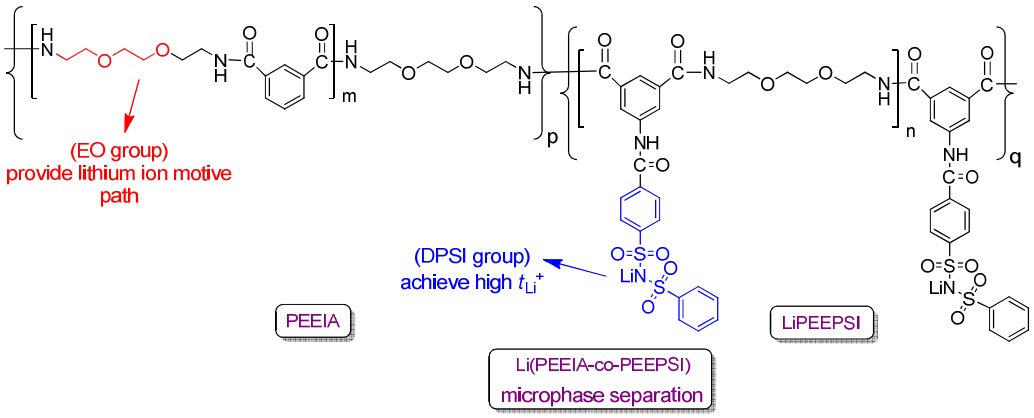

Figure 1. Chemical structure of the single ion conducting block copolymer electrolyte PEEIA-co-LiPEEPSI.

2. Experimental

2.1 Materials

P-toluenesulfonamide (≥98%) (Sigma-Aldrich), benzenesulfonchloride (99%) (Sigma-Aldrich), $KMnO_4$ (GCE), lithium hydroxide monohydrate (Sigma-Aldrich), 2,2'-(ethylenedioxy)bis(ethylamine) (98%) (Sigma-Aldrich) and PVDF-HFP (Sigma-Aldrich) were used as received. Dimethyl-5-aminoisophthalate (Sigma-Aldrich), calcium chloride (GCE) and isophthalic acid (99%) (Sigma-Aldrich) were dried overnight in a vacuum oven at 80 ^oC before use. Pyridine (Alfa-Aesar) was dried over KOH, N-methyl-2-pyrrolidone (NMP) (VWR) was dried over phosphorus (V) oxide. Triphenylphosphine (TPP) (Alfa-Aesar), analytical grade acetone, ethylene carbonate (EC) (Sigma-Aldrich), methanol, tetrahydrofuran (THF) (RCI labscan), and propylene carbonate (PC) (Sigma-Aldrich) were used as received without further purification. Cambridge Isotope Laboratories deuterated dimethyl sulfoxide (DMSO-d6) solvent was used for the NMR tests.

View Article Online
DOI: 10.1039/C4RA08709G

2.2 Synthesis of the PEEIA-co-LiPEEPSI

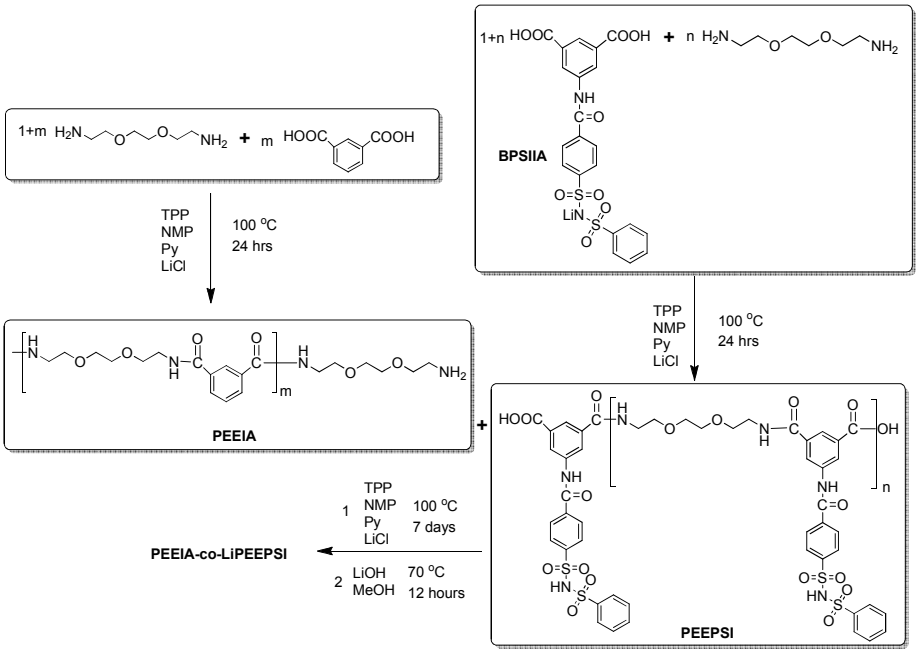

Scheme 1: Polymerization scheme of PEEIA, PEEPSI to form PEEIA-co-LiPEEPSI via a polycondensation reaction.

Synthesis of the homopolymers. The precursor, bis(phenylsulfonyl imide isophthalate amide (BPSIIA), was synthesized following the procedure described in our previous work (Supporting Information).[40] The homopolymers, poly((2,2'-ethylenedioxy) bis(ethylamine) isophthalic acid amide) (PEEIA) and lithium poly((2,2'-ethylenedioxy)bis(ethylamine) bis(phenylsulfonyl imide) isophthalate amide) (PEEPSI), were separately synthesized using the procedure described in Ref. 26. Isophthalic acid (1.1255 g, 6.667 mmol) and 2,2'-(ethylenedioxy) bis(ethylamine) (1.0374 , 7 mmol) were added into a mixture of 1.60 g of lithium chloride, 5 ml of TPP, 20 mL of NMP and 15 ml of pyridine for the synthesis of PEEIA. BPSIIA (1.1514 g, 3 mmol) and 2,2'-(ethylenedioxy) bis(ethylamine) (0.4234

View Article Online
DOI: 10.1039/C4RA08709G

g, 2.857 mmol) were added into a mixture of 1.60 g of lithium chloride, 5 ml of TPP, 20 ml of NMP and 15 ml of pyridine for the synthesis of PEEPSI. The reactions were first kept at 100 ^{o}C for 12 hours under argon atmosphere overnight. After that, an excess of additional 10 % mole of 2,2'-(ethylenedioxy)bis(ethylamine) and BPSIIA were added into the reaction mixtures, respectively. These moieties were left to reflux for another 5 hours. The hot mixtures were separately poured into 100 ml of acetone with stirring and washed repeatedly with acetone until fine powders were obtained. The lithiation of PEEPSI was carried out by an acid-base neutralization reaction with $LiOH{\cdot}H_2O$ in methanol at 70 ^{o}C for 12 hours. Upon solvent removal, LiPEEPSI was dried at 80 ^{o}C for 24 hours.

Synthesis of the block copolymer. PEEIA (0.1380 g, 0.0105 mmol) and LiPEEPSI (0.5000 g, 0.0105 mmol) were added into a mixture of 0.16 g of lithium chloride, 0.7 ml of TPP, 2 ml of NMP and 1.5 ml of pyridine in a glove box. The reaction was conducted at 100 ^{o}C under argon atmosphere for a week. After that, the mixture was poured into 60 ml of acetone to produce a pale pink precipitate. The polymer was washed continuously with acetone. The block copolymer (PEEIA-co-LiPEEPSI) was collected via vacuum filtration and dried in a vacuum oven at 80 ^{o}C for 24 hours. The molecular weights of the homopolymers and block copolymer were characterized by gel permeation chromatography (GPC) (Table 1).

View Article Online
DOI: 10.1039/C4RA08709G

Table 1. Molecular weights and PDSI of PEEIA, PEEPSI and PEEIA-co-PEEPSI.

	M_n	M_w	*PDI*
PEEIA	13,600	31,416	2.31
PEEPSI	49,271	87,512	1.77
PEEIA-co-PEEPSI	57,284	111,224	1.94

2.3 Characterizations

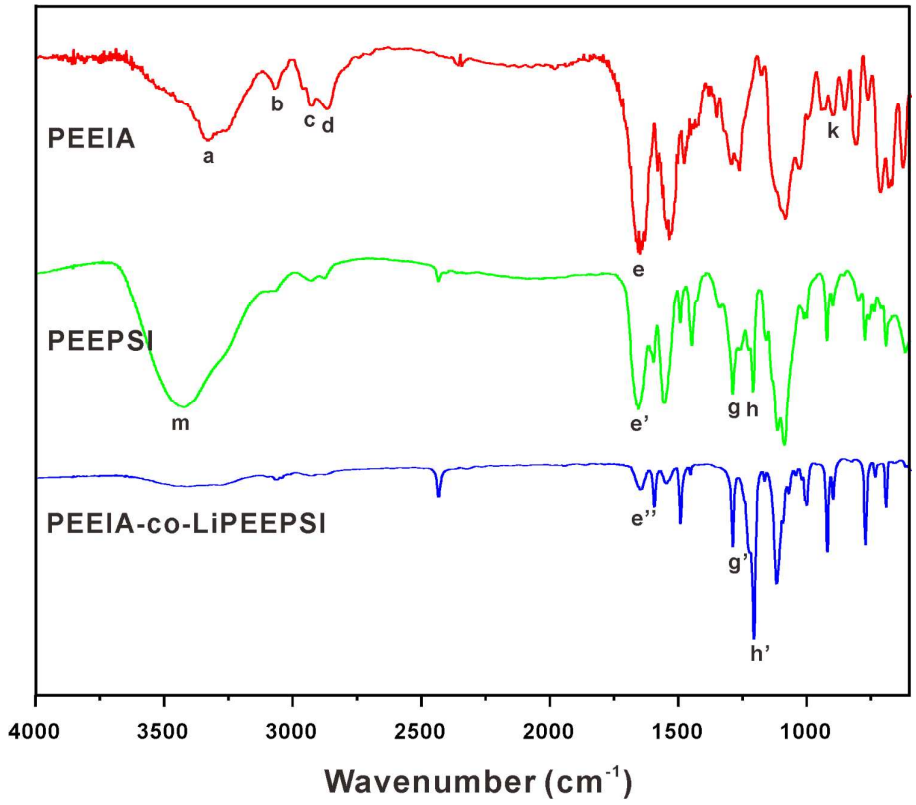

Figure 2. The FTIR spectra of the PEEIA, PEEPSI and PEEIA-co-LiPEEPSI.

The FTIR spectra of PEEIA, PEEPSI and PEEIA-co-PEEPSI are shown in Figure 2. The characteristic bands of PEEIA at 3300 cm^{-1} (a) and 893 cm^{-1} (k) indicate a presence of primary amine at the terminals of PEEIA. The broad peak of PEEPSI at around 3475 cm^{-1} (m) is assigned to the O-H bond stretch arising from the

View Article Online
DOI: 10.1039/C4RA08709G

COOH groups at the terminals of PEEPSI. The peaks at 1649 cm^{-1} (e), 1654 cm^{-1} (e') and 1649 cm^{-1} (e'') are assigned to amide C=O stretching of PEEIA, PEEPSI and PEEIA-co-PEEPSI, respectively. The peaks at 1339 cm^{-1} (g) and 1158 cm^{-1} (h) of PEEPSI and 1325 cm^{-1} (g') and 1165 cm^{-1} (h') of PEEIA-co-PEEPSI reflect the O=S=O asymmetric stretching and symmetric stretching, respectively.

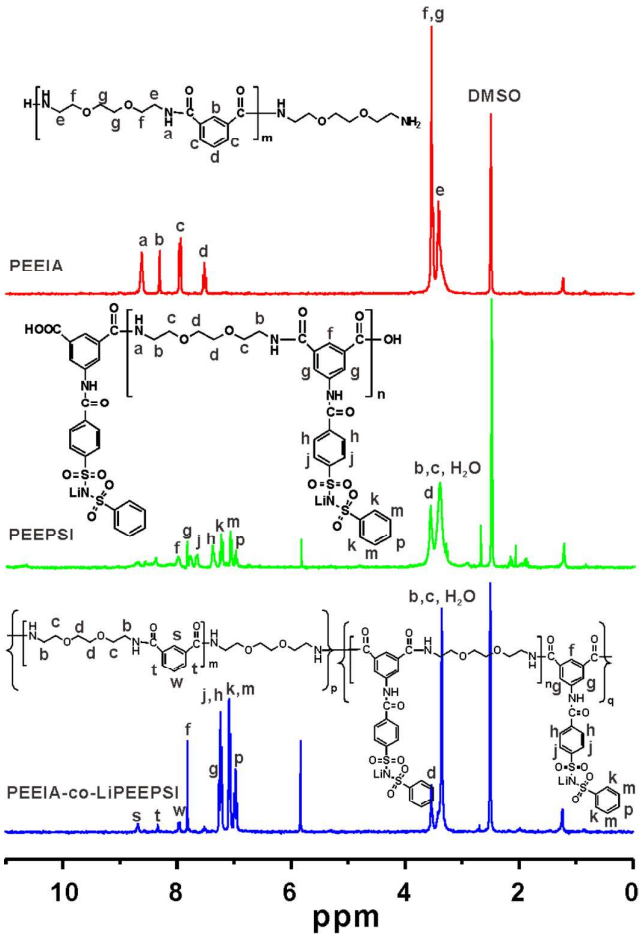

Figure 3. The ^{1}H NMR spectra of PEEIA PEEPSI and PEEIA-co-LiPEEPSI.

The $^{1}HNMR$ spectra of PEEIA, PEEPSI and PEEIA-co-LiPEEPSI are shown in Figure 3. The spectrum of PEEIA shows clearly defined peaks at 7.52 ppm, 7.96 ppm 8.31 ppm and a broader signal at 8.62 ppm whose integration ratio corresponds

View Article Online
DOI: 10.1039/C4RA08709G

well with the number of protons in the aromatic ring and the amide bond. The signals at 3.4 - 3.5 ppm correspond to the protons in 2,2'-(ethylenedioxy)bis(ethylamine). For the spectrum of PEEIA, the signals for hydrogen (H_{f-p}) on the BPSIIA segments are clearly identified and the signals at 3.4 - 3.5 ppm, corresponding to the protons in 2,2'-(ethylenedioxy)bis(ethylamine), are ready visible. All the proton signals of PEEIA and PEEPSI are observed in the spectrum of the PEEIA-co-LiPEEPSI block copolymer. Comparing the ^1H NMR spectra of PEEIA-co-PEEPSI and the homopolymers, the proton signals of the aromatic segments on PEEIA (H_{b-d}) and on the aromatic ring in PEEPSI (H_{f-p}) shift slightly to the lower frequencies upon copolymerization to form PEEIA-co-PEEPSI.

2.4 Preparation of single-ion conducting polymer electrolyte membranes (SIPEMs)

The SIPE membranes were fabricated using PVDF-HFP as a binder via a solution cast method without using a pore inducing agent. PVDF-HFP and PEEIA-co-LiPEEPSI with an equivalent mass ratio were dissolved in DMF at 80 ^oC to form a homogenous solution. The composite polymer was then casted onto a glass petri dish, which was kept at 80 ^oC for overnight for solvent evaporation. After that, the membrane was peeled off from the petri dish and transferred into a vacuum oven for overnight at 80 ^oC to remove a trace of the solvent. The dried membrane was subsequently transferred into a glove box and soaked in an EC/PC (v:v, 1:1) solvent for overnight before performing electrochemical characterization and battery performance test. The choice of organic solvent greatly influences the properties of

View Article Online
DOI: 10.1039/C4RA08709G

the electrolyte. For example, high dielectric constant of organic solvent can prompt the delocalization of the Li-ion while low viscosity of organic solvent enhances Li-ion mobility in the electrolyte.[41-45] Here the objective of the present study is to demonstrate the concept of single ion conducting block copolymer electrolytes, rather than to select an optimal solvent, for applications in lithium ion batteries. Therefore, EC/PC solution, which has been extensively used in literature,[46,47] was selected in the present work. For comparison, a blend membrane of PVDF-HFP and LiPEEPSI with an equivalent mass ratio was also prepared using the same procedure. The thickness of the membrane is in the range of 20 - 30 μm. The methods to test the properties and performance of the membranes are described in details in Supporting Information.

2.5 Battery test and fabrication of cathode film.

Battery performance was studied using a multichannel battery testing instrument Arbin BT-2000 in which the cell was charged and discharged at different C rates over the voltage range 3.8 - 2.5 V. The coin cell (CR2025 type) was made by sandwiching SIPE membrane between a lithium metal foil and a $LiFePO_4$ electrode. The cathode was prepared by casting a homogenous mixture of 75 % $LiFePO_4$, 10 % carbon black, 10 % PVDF, and 5% bis(4-carboxyl benzene benzene sulfonyl) imide (CBBSI) as a supporting electrolyte in NMP solvent onto an aluminium foil. The cathode was subsequently dried in a vacuum oven at 80 ^oC overnight.

3. Results and Discussion

View Article Online
DOI: 10.1039/C4RA08709G

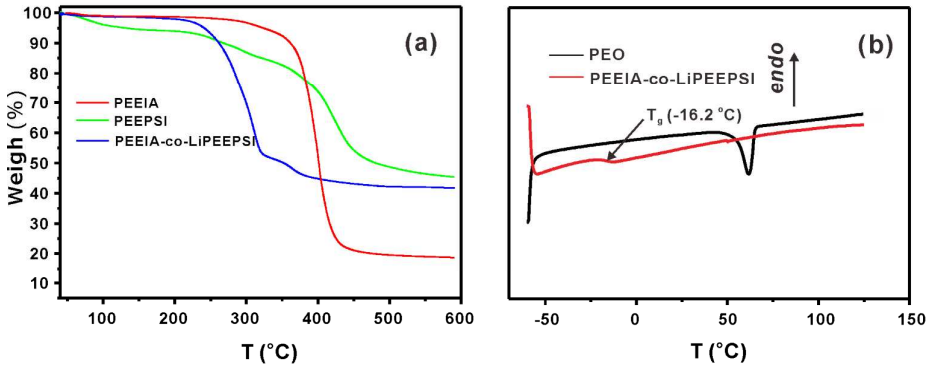

Figure 4. (a) The TG curve and (b) DSC curves of the PEEIA-co-LiPEEPSI SIPE.

The thermal stability of the PEEIA-co-LiPEEPSI membrane was measured with TGA and DSC techniques (Figure 4). The membrane remains stable until 220 ^{o}C, at which degradation occurs. The degradation temperature is substantially higher than the conventional operation temperature range of lithium ion batteries (Figure 4a). The DSC curve shown in Figure 4b indicates that PEEIA-co-LiPEEPSI exhibits a low glass transition temperature (T_g) of -16.2 ^{o}C, which is attributed to the increase of the randomness of the copolymer due to the introduction of the flexible EO leads into the PEEIA-co-LiPEEPSI copolymer.[48] The T_g is higher than that of PEO (-59 ^{o}C), likely resulting from the hydrogen bonding interaction between amide groups. The lithium ion mobility can still be comparable to that of PEO based polymer membranes at room temperature duo to the low T_g of PEEIA-co-LiPEEPSI.

View Article Online
DOI: 10.1039/C4RA08709G

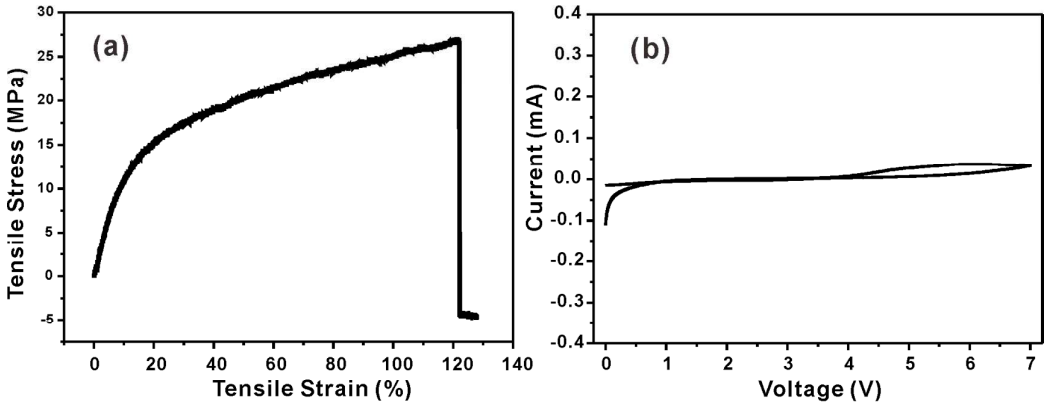

Figure 5. (a) The mechanical stability and (b) electrochemical stability of the PVDF-HFP/PEEIA-co-LiPEEPSI membrane.

Figure 5 shows the mechanical and electrochemical stabilities of the PVDF-HFP/PEEIA-co-LiPEEPSI membrane. The PVDF-HFP/PEEIA-co-LiPEEPSI membrane displays an excellent mechanical strength of 27 MPa (Figure 5a), substantially higher than the corresponding values (ca. 20 MPa) of most PVDF-HFP blended SIPE membranes.[38] This result indicates that the PVDF-HFP/PEEIA-co-LiPEEPSI membrane is both mechanically and dimensionally stable, which is highly beneficial for prolonging the cyclic life of batteries. The electrochemical stability of the PVDF-HFP/PEEIA-co-LiPEEPSI membrane was determined via measurement of cyclic voltammetry (CV) on a Li|PVDF-HFP/PEEIA-co-LiPEEPSI|Stainless steel (SS) cell with the CV curve shown in Figure 5b.[49] The high electrochemical stability up to 4.3 V suggests that the PVDF-HFP/PEEIA-co-LiPEEPSI membrane might be useful for batteries that need a wider electrochemical window than what can be offered by conventional liquid electrolytes. We further measured the lithium ion transference number of the

View Article Online
DOI: 10.1039/C4RA08709G

PVDF-HFP/PEEIA-co-LiPEEPSI membrane (t_{Li^+}) in a Li|PVDF-HFP/PEEIA-co-LiPEEPSI|Li symmetric cell at room temperature using the steady-state current method (Figure S3). The measured values required to derive t_{Li^+} are summarized in Table S1. The value of t_{Li^+} of the PVDF-HFP/PEEIA-co-LiPEEPSI membrane was found to be 0.91, substantially higher than that of conventional liquid electrolytes (< 0.3) and similar to those of the reported SIPEs.[20]

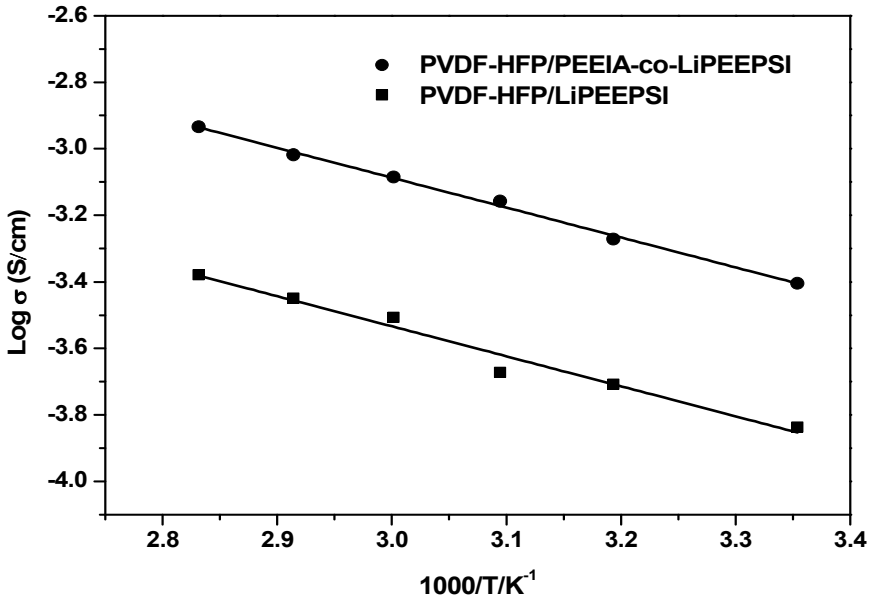

Figure 6. The ionic conductivities of the PVDF-HFP/PEEIA-co-LiPEEPSI membranes and the PVDF-HFP/ LiPEEPSI membranes vs. the inverse of temperature.

The temperature dependence of the ionic conductivity of the PVDF-HFP/PEEIA-co-LiPEEPSI membrane is depicted in Figure 6. For comparison, the conductivity of the PVDF-HFP/LiPEEPSI membrane is also shown here. The ionic conductivity of the PVDF-HFP/PEEIA-co-LiPEEPSI membrane is 3.39×10^{-4} S

View Article Online
DOI: 10.1039/C4RA08709G

cm^{-1} at room temperature and reaches to 1.16×10^{-3} S cm^{-1} at 80 ^{o}C. In contrast, the ionic conductivity of the PVDF-HFP/LiPEEPSI membrane is 1.46×10^{-4} S cm^{-1} at room temperature and 4.18×10^{-4} S cm^{-1} at 80 ^{o}C, about three times lower than the value of the PVDF-HFP/PEEIA-co-LiPEEPSI membrane. The excellent ionic conductivity of PEEIA-co-LiPEEPSI is chiefly attributed to the contribution of the EO segments in the polymer backbone with an additional contribution from the porous morphology of the material, which enables a high solvent uptake to enhance ion mobility without compromising dimensional stability of the membrane.

It should be noted here that blending the nonconductive PVDF-HFP with PEEIA-co-LiPEEPSI would inevitably affect the ion conductivity of the membrane. Rani et al. showed that for PVDF-HFP blended GPE membranes, ion conductivity increases as PVDF-HFP content decreases,[50] which is not surprising since the number of charge carriers in a membrane with a low content of PVDF-HFP is higher. We observed a similar phenomenon in our experiments and made significant effort to use only a minimum amount of PVDF-HFP in the membrane to enhance ionic conductivity while maintaining sufficient mechanical strength. The optimal ratio of PVDF-HFP to PEEIA-co-LiPEEPSI was found to be 1:1.

The high solvent uptake (141 wt. %) is evidenced from the surface SEM images of the PVDF-HFP/PEEIA-co-LiPEEPSI membrane shown in Figure 7 (a and b). Importantly, the continuous ion conducting channels are well established upon microphase separation, which is imperative for Li-ion batteries. In contrast, the

View Article Online
DOI: 10.1039/C4RA08709G

PVDF-HFP/LiPEEPSI membrane exhibits essentially no porosity as clearly shown in Figure 7c.

In general, the morphology of the blend membranes is affected by the compatibility of the polymers.[29] For example, the aliphatic PVDF-HFP is compatible with the aliphatic segments but not compatible with the aromatic segments in the polymer electrolyte. As a consequence, the morphology of the PVDF-HFP/LiPEEPSI membrane is not porous (Figure 7c) while the PVDF-HFP/PEEIA-co-LiPEEPSI membrane exhibits pores (Figure 7b).

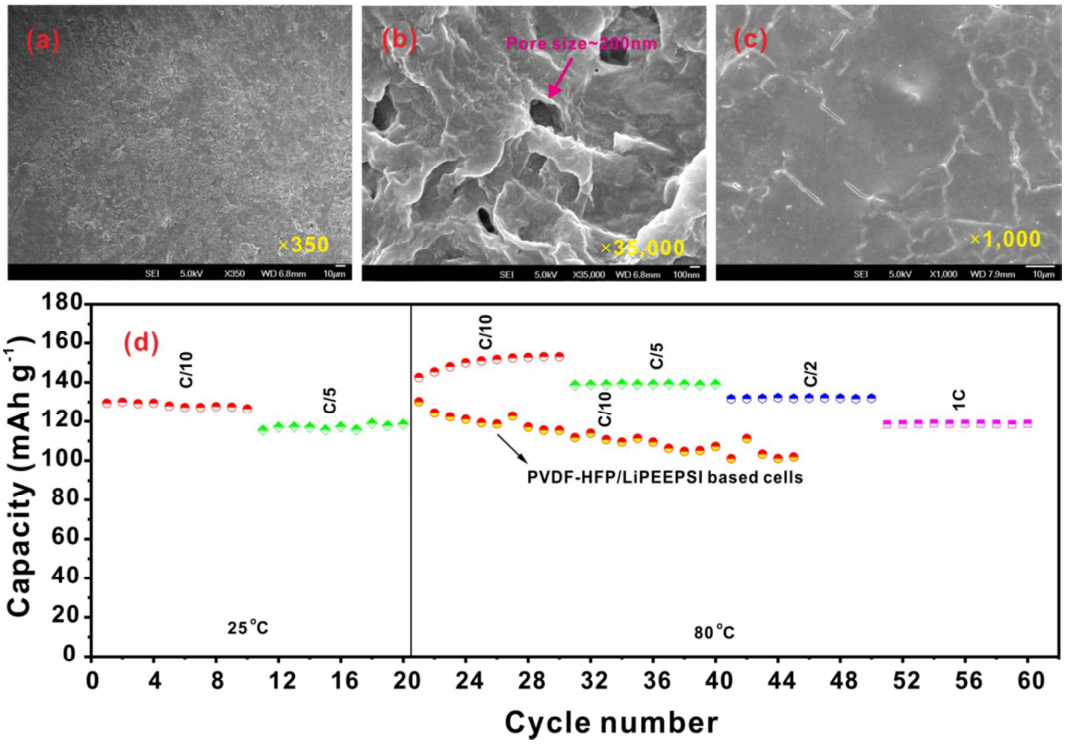

Figure 7. The SEM images of the PVDF-HFP/PEEIA-co-LiPEEPSI membrane: (a) ×350, (b) ×35,000; the SEM image of the surface morphology of the PVDF-HFP/LiPEEPSI membrane (c) ×1,000. The cycle performance of the prototype Li|PVDF-HFP/SIPE membranes|$LiFePO_4$ cells (d).

View Article Online
DOI: 10.1039/C4RA08709G

The battery performance of the prepared SIPE membranes in Li-ion batteries was investigated at various C-rates at 25 ^{o}C and 80 ^{o}C, respectively. Figure 7d shows the discharge capacity vs. the cycle numbers of the battery cells. Unlike most of the SIPE based batteries,[21,27,38] the battery of the Li|PVDF-HFP/PEEIA-co-LiPEEPSI|$LiFePO_4$ is operative at room temperature and the discharge capacity was found to be 130 mAh g^{-1} at 0.1 C and 118 mAh g^{-1} at 0.2 C. At 80 ^{o}C, the performance was significantly improved both from discharge capacity and C-rate and the discharge capacity becomes 150 mAh g^{-1} at 0.1 C and 140 mAh g^{-1} at 0.2 C, close to the theoretical capacity. More remarkably, the battery maintains a high discharge capacity of 130 mAh g^{-1} at 0.5 C and 120 mAh g^{-1} at 1 C, respectively, without obvious capacity fading after 60 cycles. In comparison, a battery equipped with the PVDF-HFP/LiPEEPSI membrane is only operative at an elevated temperature and a low C-rate of 0.1 C with a much lower average discharge capacity of 110 mAh g^{-1} (Figure 7). In addition, the battery displays unstable cycle performance. The performance of both batteries suggests that the microstructure of SIPE membranes can profoundly influence operability of battery cells. Indeed, the superior performance of the PVDF-HFP/PEEIA-co-LiPEEPSI membrane is largely attributed to the nicely formed continuous ion transport channels arising from its macroporous morphology. In contrast, the PVDF-HFP/LiPEEPSI membrane without proper porosity prevents establishment of continuous ion transport channels and thus leads to inferior performance.

4. Conclusions

View Article Online
DOI: 10.1039/C4RA08709G

A single ion block copolymer (PEEIA-co-PEEPSI) was successfully prepared via copolymerization of the two carefully designed homopolymers, PEEIA and PEEPSI upon a lithiation reaction with $LiOH{\cdot}H_2O$. The homopolymers and the copolymer were characterized using FTIR, ^{1}HNMR, GPC, TGA and DSC spectroscopic techniques. Subsequently, a PEEIA-co-LiPEEPSI based SIPE membrane was fabricated by blending with a PVDF-HFP binder using a solution cast method. The physicochemical properties of the membrane were then systematically tested. The PEEIA-co-LiPEEPSI membrane displays good thermal stability up to 220 ^oC, a low T_g of -16.9 ^oC and a melting point higher than 125 ^oC. Importantly, the membrane exhibits a macroporous structure with a high solvent retention capacity up to 141 wt.%, leading to high ionic conductivity of 3.39×10^{-4} S cm^{-1} at room temperature and 1.16×10^{-3} S cm^{-1} at 80 ^oC. In addition, the material is electrochemically stable with a wide electrochemical window up to 4.3 V. The measured ion transference number is 0.91, substantially higher than the value found in dual-ion based electrolytes. The membrane displays an excellent mechanical strength up to 27 MPa. More remarkably, a battery assembled with the PVDF-HFP/PEEIA-co-LiPEEPSI membrane displays outstanding performance both at room temperature and 80 ^oC with a highly stable discharge capacity at various C-rates. Even at 1 C, the average discharge capacity still maintains at 120 mAh g^{-1} without performance fading after 60 cycles In comparison, a battery equipped with the PVDF-HFP/LiPEEPSI membrane with essentially no proper porosity and ion transport channels in the polymer matrix displays only a modest discharge capacity of

View Article Online
DOI: 10.1039/C4RA08709G

110 mAh g^{-1} at 80 ^{o}C and 0.1 C. The results underscore the fundamental importance of the microstructure of polymer electrolytes in battery performance enhancement and suggest ways to improve the design of new electrolyte materials for development of better battery devices with high longevity and high discharge capacity.

ACKNOWLEDGMENT

The authors gratefully acknowledge support of a Start-up grant from NUS, a POC grant from National Research Foundation of Singapore, Singapore–Peking-Oxford Research Enterprise (SPORE), and a DSTA grant and a grant from the National Natural Science Foundation of China (No. 21233006).

View Article Online
DOI: 10.1039/C4RA08709G

References

1 W. H. Meyer, *Adv Mater.* 1998, **10**, 439-448.
2 L.-Y. Huang, Y.-C. Shih, S.-H. Wang, P.-L. Kuo and H. Teng, *J Mater Chem A.* 2014, **2**, 10492-10501.
3 L.-Q. Fan, J. Zhong, J.-H. Wu, J.-M. Lin and Y.-F. Huang, *J Mater Chem A.* 2014, **2**, 9011-9014.
4 P. Wang, S. M. Zakeeruddin, J. E. Moser, M. K. Nazeeruddin, T. Sekiguchi and M. Gratzel, *Nat Mater.* 2003, **2**, 402-407.
5 A. Manuel Stephan, *Euro Polym J.* 2006, **42**, 21-42.
6 H. Hu, W. Yuan, H. Zhao, G. L. Baker, *J Polym Sci Pol Chem.* 2014, **52**, 121-127.
7 J. B. Goodenough, Y. Kim, *Chem Mat.* 2009, **22**, 587-603.
8. A. Stephan, *Euro Polym J.* 2006, **42**, 2-42.
9 D. R. MacFarlane, J. Huang and M. Forsyth, *Nature.* 1999, **402**, 792-794.
10 N. Kamaya, K. Homma, Y. Yamakawa, M. Hirayama, R. Kanno, M. Yonemura, T. Kamiyama, Y. Kato, S. Hama, K. Kawamoto and A. Mitsui, *Nat Mater.* 2011, **10**, 682-686.
11 Y. Zhang, Y. Sun, G. Xu, W. Cai, R. Rohan, A. Lin and H. Cheng, *Energy Technology.* 2014. 2014, **2**, 643-650.
12 R. Bouchet, S. Maria, R. Meziane, A. Aboulaich, L. Lienafa, J.-P. Bonnet, T. N. T. Phan, D. Bertin, D. Gigmes, D. Devaux, R. Denoyel and M. Armand, *Nat Mater.* 2013, **12**, 452-457.
13 F. B. Dias, L. Plomp and J. B. J. Veldhuis, *J Power Sources.* 2000, **88**, 169-191.
14 J. H. Cao, B. K. Zhu, Y. Y. Xu, *J Membrane Sci*. 2006, **281**, 446-453.
15 F. Boudin, X. Andrieu, C. Jehoulet, I. I. Olsen, *J Power Sources*. 1999, **81-82**, 804-807.
16 S. S. Zhang, *J Power Sources.* 2007, **164**, 351-364.
17 Y. Saito, H. Kataoka and A. M. Stephan, *Macromolecules.* 2001, **34**, 6955-6958.
18 E. Quartarone and P. Mustarelli, *Chem Soc Rev.* 2011, **40**, 2525-2540.
19 J. N. Chazalviel, *Phys Rev A.* 1990, **42**, 7355-7367.
20 R. Meziane, J.-P. Bonnet, M. Courty, K. Djellab and M. Armand, *Electrochim Acta.* 2011, **57**, 14-19.
21 X. G. Sun and J. B. Kerr, *Macromolecules.* 2006, **39**, 362-372.
22 X. Wang, Z. Liu, C. Zhang, Q. Kong, J. Yao, P. Han, W. Jiang, H. Xu and G. Cui, *Electrochim Acta.* 2013, **92**, 132-138.
23 W. Cai, Y. Zhang, J. Li, Y. Sun and H. Cheng, *Chemsuschem.* 2014, **7**, 1063-1067.
24 Y. Zhang, G. Xu, Y. Sun, B. Han, T. B. W. T, Z. Chen, R. Rohan and H. Cheng, *RSC Adv.* 2013, **3**, 14934-14937.
25 Y. Zhang, R. Rohan, Y. Sun, W. Cai, G. Xu, A. Lin and H. Cheng, *RSC Adv.* 2014, **4**, 21163-21170.
26 R. Rohan, Y. Sun, W. Cai, K. Pareek, Y. Zhang, G. Xu and H. Cheng, *J Mater Chem A.* 2014, **2**, 2960-2967.
27 Y. Sun, R. Rohan, W. Cai, X. Wan, K. Pareek, A. Lin, Y. Zhang and H. Cheng, *Energy Technology.* 2014, **2**, 698-704.

View Article Online
DOI: 10.1039/C4RA08709G

28 Y. Zhu, S. Xiao, Y. Shi, Y. Yang and Y. Wu, *J Mater Chem A.* 2013, **1**, 7790-7797.
29 I. M. Zorin, N. A. Zorina, A. Y. Bilibin, *Polym Sci Ser A.* 2010**, 52**, 150-159.
30 Q. Shi, M. Yu, X. Zhou, Y. Yan and C. Wan, *J Power Sources.* 2002, **103**, 286-292.
31 P. P. Soo, B. Huang, Y.-I. Jang, Y.-M. Chiang, D. R. Sadoway and A. M. Mayesz, *J Electrochem Soc.* 1999, **146**, 32-37.
32 Y. Zhang, J. Ting, R. Rohan, W. Cai, J. Li, G. Xu, Z. Chen, A. Lin and H. Cheng, *J Mater Sci.* 2014, **49**, 3442-3450.
33 M. Watanabe, Y. Suzuki and A. Nishimoto, *Electrochim Acta.* 2000, **45**, 1187-1192.
34 D. Benrabah, S. Sylla, F. Alloin, J. Y. Sanchez and M. Armand, *Electrochim Acta.* 1995, **40**, 2259-2264.
35 K. Onishi, M. Matsumoto, Y. Nakacho and K. Shigehara, *Chem Mater.* 1996, **8**, 469-472.
36 Y. Tada, M. Sato, N. Takeno, Y. Nakacho and K. Shigehara, *Chem Mater.* 1994, **6**, 27-30.
37 S. W. Feng, D. Y. Shi, F. Liu, L. P. Zheng, J. Nie, W. F. Feng, X. J. Huang, M. Armand and Z. B. Zhou, *Electrochim Acta.* 2013, **93**, 254-263.
38 K. Matsumoto and T. Endo, *J Polym Sci Polym Chem.* 2011, **49**, 1874-1880.
39 X. Wang, Z. Liu, C. Zhang, Q. Kong, J. Yao, P. Han, W. Jiang, H. Xu and G. Cui, *Electrochim Acta.* 2013, **92**, 132-138.
40 J. Li, W. Cai, Y. Zhang and H. Cheng, *Energy Technology.* 2014, **2**, 685–691.
41 M. Doyle, M. E. Lewittes, M. G. Roelofs, S. A. R. E. Perusich, Lowrey, *J Membr Sci.* 2001, **184**, 257-273.
42 S. Sachan, C. A. Ray, S. A. Perusich, R. Hall and S. Sachun, *Polym. Eng. Sci.*, 2002, **42**, 1469.
43 K. D. Kreuer, A. Wohlfarth, C. C. de Araujo, A. Fuchs, J. Maier, *Chemphyschem*, 2011, **12**, 2558-2560.
44 S. Srivastava, J. L. Schaefer, Z. Yang, Z. Tu, L. A. Archer, *Adv. Mater*. 2014, **26**, 201-234.
45 Z. Jin, K. Xie, X. Hong, *J Mater Chem A.* 2013, **1**, 342-347.
46 E. H. Kil, K. H. Choi, H. J. Ha, S. Xu, J. A. Rogers, M. R. Kim, Y. G. Lee, K. M. Kim, K. Y. Cho, S. Y. Lee, *Adv Mater.* 2013, **25**, 1395-1400.
47 Z. Cai, Y. Liu, S. Liu, L. Li, Y. Zhang, *Enery Environ Sci.* 2012, **5**, 5690.
48 H. Hu, W. Yuan, L. Lu, H. Zhao, Z. Jia, G. L. Baker, *J Polym Sci Pol Chem*. 2014, **52**, 2104-2110.
49 A. Ghosh , C. S. Wang, P. Kofinas, *J Electrochem Soc.* **2010**, 157, A846-A849.
50 M. Rani,R. Babu, S. Rajendran, *Int J ChemTech Res.* 2013, **5**, 1724-1732.

Electronic Supplementary Material (ESI) for RSC Advances.

Design and synthesis of a single ion conducting block copolymer electrolyte with multifunctionality for lithium ion batteries

Yunfeng Zhang,[a,b] Corina Anrou Lim,[b] Weiwei Cai,[a] Rupesh Rohan,[a] Guodong Xu,[a] Yubao Sun,[b] and Hansong Cheng[a,b*]

[a]Department of Chemistry, National University of Singapore, 3 Science Drive 3, Singapore 117543

[b]Sustainable Energy Laboratory, China University of Geosciences Wuhan, 388 Lumo RD, Wuhan 430074, China

E-mail: chmch@nus.edu.sg

1. Synthesis of bis(phenylsulfonyl imide) isophthalate amide (BPSIIA)

1.1. Synthesis of the 4-carboxyl benzene benzene sulphonyl imide (CBBSI)

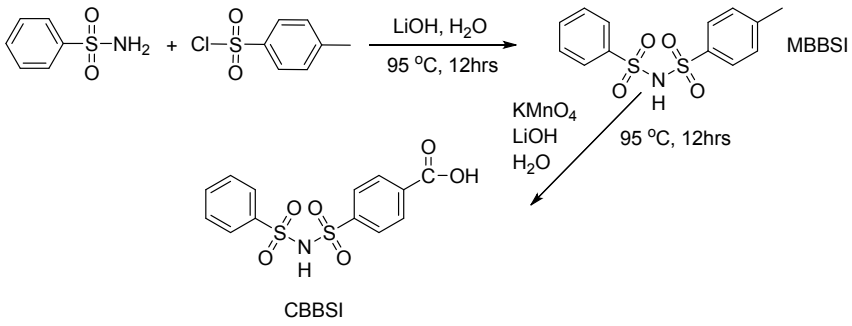

Scheme S1: Synthesis of 4-methyl benzene benzene sulfonyl imide (MBBSI) and 4-carboxyl benzene benzene sulfonyl imide (CBBSI).

Synthesis of the 4-methyl benzene benzene sulphonyl imide (MBBSI). The 4-carboxyl benzene benzene sulfonyl imide (CBBSI) was synthesized according to the procedure described by our previous works (Scheme S1).[1] P-toluenesulfonamide (34.244 g, 200 mmol) and sodium hydroxide (8.450 g, 210 mmol) were firstly dissolved in deionized water at 90 °C. Benzenesulfonyl chloride (17.662 g, 100 mmol) was then added into the solution within 2 hours followed by another 12 hours at 90 °C for completely reaction. The pH value of the reaction solution was adjusted the pH to 7 using dilute hydrochloric acid at 50 °C followed by stirring for another 12 hours. After the excessive p-toluenesulfonamide was removed by filtration, the row product was precipitated by adjusting the pH value of the filtrate to 1 using concentrated hydrochloric acid. The white precipitate was collected via vacuum filtration and dried in the oven at 80 °C. The final product was purified by recrystallization using deionized water. The yield was 59.1%. ^{1}HNMR (DMSO-d_6): 7.70, 7.67 (d, 2H), 7.58, 7.55 (d, 2H), 7.49, 7.47, 7.45, 7.42 (m,

3H), 7.23, 7.22 (d, 2H) and 2.34 (s, 3H) (Fig. S1a), ESI-MS $[M-H]^-$ at m/z 311.38 calculated for $C_{13}H_{13}NO_4S_2$.

Synthesis of the 4-carboxyl benzene benzene sulphonyl imide (CBBSI): 4-carboxyl benzene benzene sulfonyl imide (CBBSI) was obtained by oxidizing the methyl group of the MBBSI into carboxyl acid group by using potassium permanganate ($KMnO_4$). MBBSI (15.174 g, 48.7 mmol), lithium hydroxide monohydrate (2.045 g, 48.73 mmol) was completely dissolved in 300 mL of deionized water at 95 ^oC. $KMnO_4$ (19.252 g, 121.8 mmol) was added into the solution over 2 hours and left the solution for overnight at 95 ^oC. Manganese oxide and unreacted potassium permanganate were removed by vacuum filtration. The final product was precipitated by adding concentrated hydrochloric acid into the filtrate and the final desired product was acidified for 5 times to completely replace K^+ by H^+ with a yield of 82.6 %. ^{1}HNMR (DMSO-d_6): 7.92, 7.90 (d, 2H), 7.76, 7.73 (d, 2H), 7.66, 7.64 (d, 2H), 7.43, 7.41, 7.38, 7.36, 7.34 (m, 3H) (Fig. S1b), ESI-MS $[M-H]^-$ at m/z 341.36 calculated for $C_{13}H_{11}NO_6S_2$.

1.2. Synthesis of the bis(phenylsulfonyl imide dimethyl-5-isophthalate amide (BPSIIA)

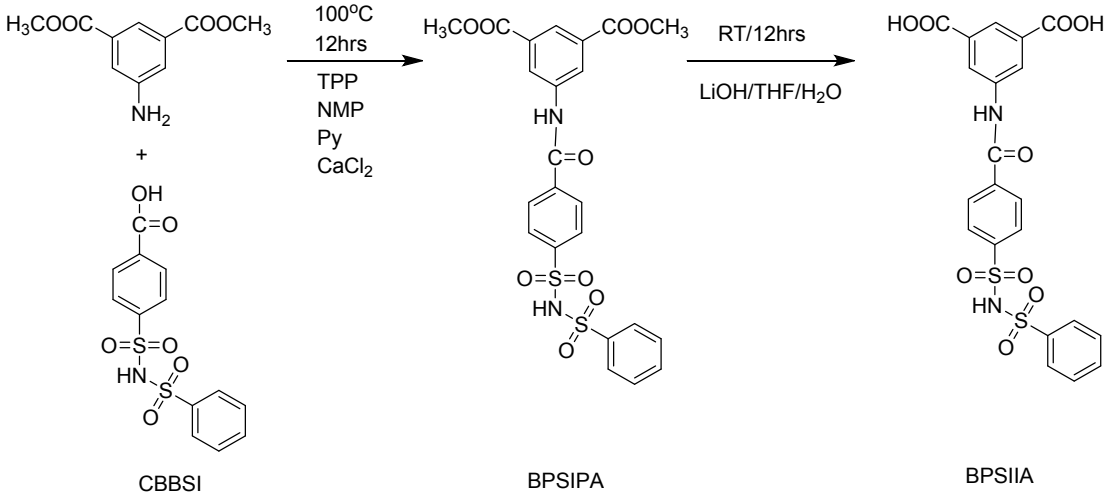

CBBSI BPSIPA BPSIIA

Scheme S2: Synthesis of bis(phenylsulfonyl imide) isophthalate amide (BPSIIA).

Synthesis of the bis(phenylsulfonyl imide dimethyl-5-isophthalate amide (BPSIPA). The bis(phenylsulfonyl imide) isophthalate amide (BPSIIA) was synthesized by following the synthesis of the precursor bis(phenylsulfonyl imide dimethyl-5-isophthalate amide (BPSIPA) (Scheme S2). CBBSI (3.4136 g, 10 mmol), dimethyl-5-aminoisophthalate (2.092 g, 10 mmol), calcium chloride (2.80 g, 25 mmol) and TPP (2.6 ml, 20mmol) were added into a mixture of NMP (10 ml) and pyridine (7.5 ml) in an argon-filled glove box. The reaction was then transferred into fumehood and connected to argon atmosphere. The reaction was kept at 100 ^{o}C for 12 hours with stirring and poured into 80 ml cold methanol to precipitate out the product. The white precipitate (BPSIPA) was continuously washed with methanol and deionized water. The product was dried in vacuum oven at 80 ^{o}C for overnight. The yield was 95 %. ^{1}HNMR (DMSO-d_6): 10.76 (S, 1H), 8.83, 8.81 (d, 1H), 8.75 (s, 2H), 8.23(s, 1H), 8.03, 8.01, 8.98 (t, 2H), 7.82 (s, 2H), 7.70, 7.68 (d, 2H), 7.41 (s, 2H), 2.49(s, 6H) (Fig. S2a), ESI-MS $[M-H]^-$ at m/z 531.53 calculated for $C_{23}H_{19}N_2O_9S_2$.

Synthesis of the bis(phenylsulfonyl imide isophthalate amide (BPSIIA). BPSIPA (14.867 g, 27.91 mmol) was dissolved in a mixture of 400 mL THF and 80 mL of water under stirring. $LiOH{\cdot}H_2O$ (4.883 g, 91.70 mmol) was dissolved in water (25 ml) and then added into the above solution dropwise under stirring. Adjust pH of the solution to 7 with dilute hydrochloric acid. THF was removed by rotavaporation under reduced pressure. The reaction was kept at room temperature for 12 hrs. After reaction, the pH of the solution was firstly adjusted to be neutral and the solvents were removed under reduced pressure. The residue was redissolved in water, the product was generated by acidified the solution to pH=1 using aqueous HCl. The precipitate was filtered and washed with a small amount of water. The final product (12.9 g) was obtained after

dried at 100 ^{o}C for 24 hrs. The yield was 92 %. ^{1}HNMR (DMSO-d_6): 10.68 (S, 1H), 8.90, 8.88 (d, 1H), 8.68 (s, 2H), 8.23(s, 1H), 8.02, 8.00, 8.97 (t, 2H), 7.81, 7.79 (d, 2H), 7.70, 7.68 (d, 2H), 7.42, 7.41, 7.38 (t, 2H) (Fig. S2b), ESI-MS $[M-H]^-$ at m/z 503.01 calculated for $C_{21}H_{15}N_2O_9S_2$.

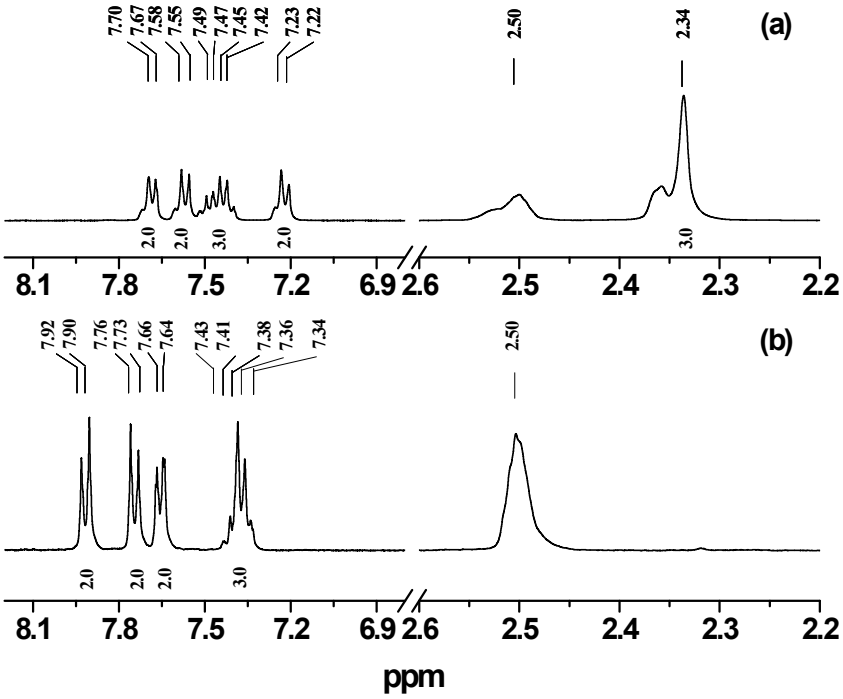

Figure S1. ^{1}H NMR spectra of MBBSI (a) and CBBSI (b).

The ^{1}H NMR spectra of the MBBSI and CBBSI are shown in Figure S1. It displays clear defined peaks with the correct integration ratio corresponding well with the number of protons in the respective compounds. The absence of a signal at 2.34 ppm in CBBSI (Figure S1b), which was assigned to the methyl group in MBBSI (Figure S1a), suggests that the MBBSI was successfully oxidised to yield CBBSI.

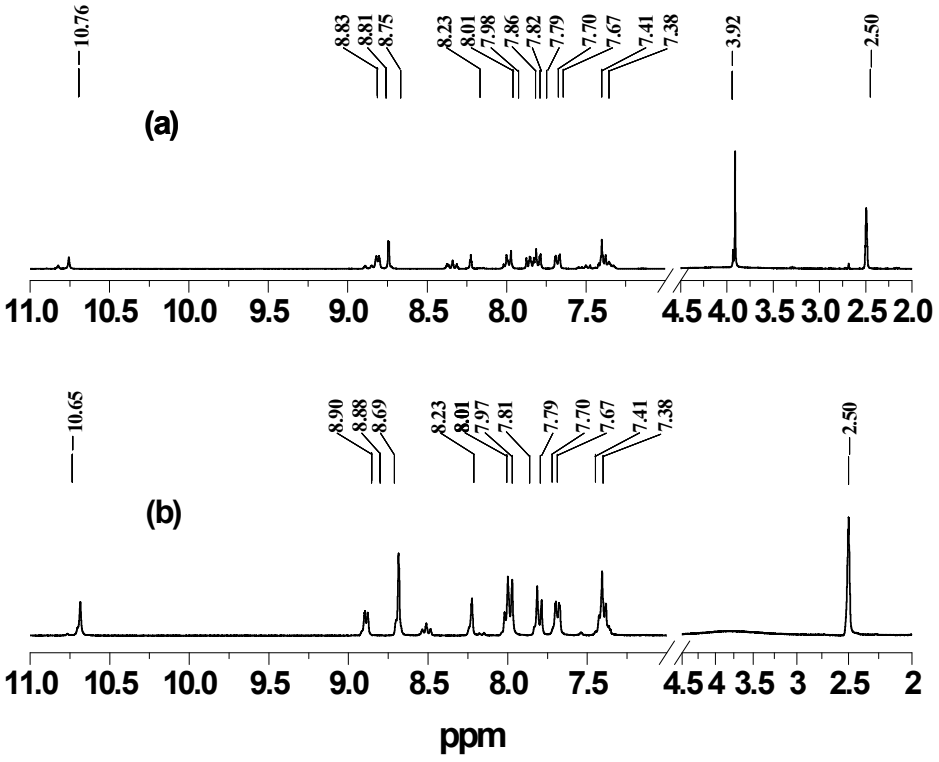

Figure S2. ^{1}H NMR spectra of BPSIPA (a) and BPSIIA (b).

The ^{1}H NMR spectra of the BPSIPA and BPSIIA are shown in Figure S2. It displays clear defined peaks with the correct integration ratio corresponding well with the number of protons in the respective compounds. The absence of the signal at 3.92 ppm in BPSIIA (Figure S2b) corresponding to the methyl group in BPSIPA (Figure S2a) suggest that BPSIPA was successfully hydrolysed to yield BPSIIA.

2. Methods

^{1}H NMR spectra of all synthesized materials were recorded on Bruker AV300 using DMSO-D6 solvent. FTIR spectra were recorded using Bio-Rad Excalibur FTIR spectrometer in the 400-4000 cm^{-1} frequency range and spectral resolution of 4. The individual polymers were mixed with KBr and made into a plate. Molecular weight and polydispersity index (PDSI) were measured using GPC using THF as an eluent. The enthalpy were analyzed using TA Instrument 2920. This analysis was performed under nitrogen atmosphere at a heating rate of 10 ^{o}C/min.

Thermal gravimetric analysis (TGA) of blended PEEIA-co-LiPEEPSI) was performed on SDT TA Instruments 2960 Simultaneous DTA-TGA, at 10.00 ^{o}C/min ramp up to 800 ^{o}C under nitrogen atmosphere. Powder XRD was performed on D5005 Bruker AXS diffractometer using sample size of 70 - 110 mg and Cu-Kα radiation (λ = 1.5410 nm) as the source at 40 kV voltage in the scanning range 1.4^{o} - 60^{o} at room temperature. Surface morphology of the blended polymer was studied using JEOL JSM-6701F field emission scanning electron microscopy. The sample was imaged after being sputter-coated with platinum. Tensile strength and tensile strain of SIPE was measured using Instron 5544 at room temperature, with an elongation rate of 1.00mm/min and sensitivity set at 40%. The membranes were measured according to ASTM D882, REF ASTM.

The amount of solvent uptake is calculated by Equation (3):

$$\eta = \frac{W_{wet} - W_{dry}}{W_{dry}} \times 100\% \qquad (1)$$

where W_{dry} and W_{wet} are the weight of the membrane before and after the absorption of EC/PC solvent.

High solvent uptake of 141% as seen in Table 3 was attributed to the high porosity of Li(PEEIA-co-PEEPSI)/PVDF-HFP with pore size of 200 nm as shown in 11 (c). High solvent uptake is essential for forming high ionic conducting SIPE.

The electrochemical stability of the SIPE membrane was determined using the CHi instrument by performing cyclic voltammetry (CV) in a sandwich cell using two stainless-steel electrodes as a working electrode and a counter electrode in the voltage range of 1.5 - 7 volts and at a scan rate of 0.2 mV s^{-1}.[2] In order to obtain a more accurate measurement of electrochemical stability, a slow

scan rate was used. Lithium ion transference number (t_{Li+}) was measured using a Li|SIPE membrane|Li battery cell. The cell was subjected to a combination of AC impedance and DC polarization method described by Evans et al. [58] lithium ion transference number was calculated using Equation (2):

$$t_{Li+} = \frac{I_s(\Delta V - I_o R_o)}{I_o(\Delta V - I_s R_s)} \qquad (2)$$

Where ΔV is the potential applied across the cell; I_o and I_s are the initial and steady-state current determined by DC polarization; R_o and R_s are the initial and steady-state resistances of the passivation layers on the Li electrode determined by AC impedance. Ionic conductivity of the SIPE membrane was measured by means of Electrochemical Impedance Spectroscopy (EIS) using Zahner electrochemical workstation model, PGSTAT, with the EIS module over a frequency range 4×10^6 to 1 Hz and an oscillating voltage of 5 mV. The electrolyte membrane was placed in a stainless steel cylindrical device of 1.5 cm diameter. The device was left in the 80 ^oC oven overnight before taking measurements to ensure maximum contact between the membrane and the device. Nyquist plot of imaginary vs real impedance were obtained and fitted with Simulated Impedance Measurement (SIM) software: The ionic conductivities were obtained by fitting the measured resistance into Equation (1):

$$\sigma = \frac{l}{AR} \qquad (3)$$

where σ is the ionic conductivity; l is the membrane thickness; A is the area of the membrane; R is the resistance obtained from the Nyquist plot.

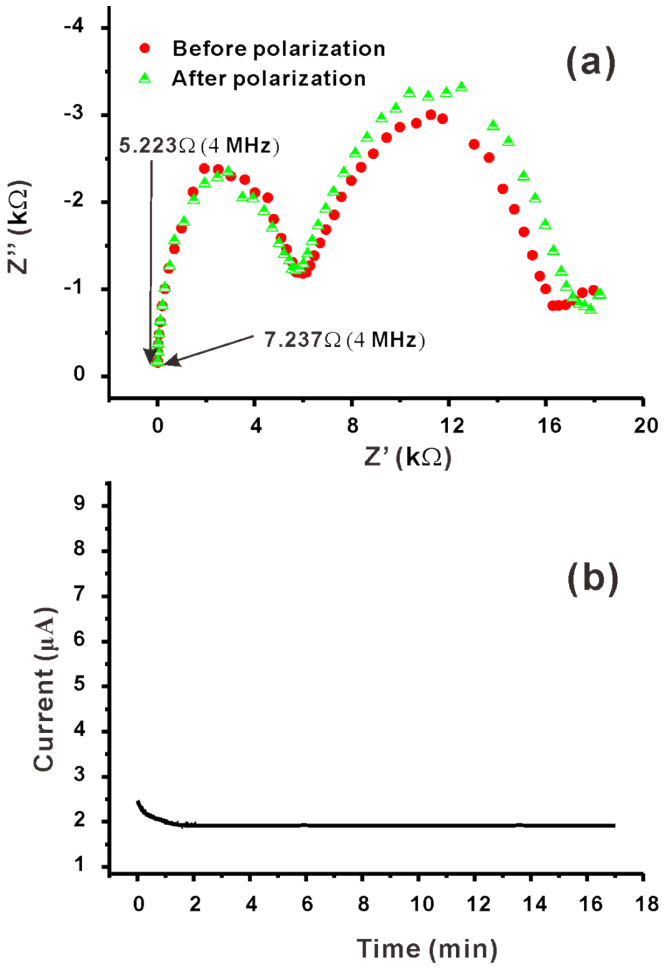

Figure S3. Impedance spectra (a) and time dependence response of DC polarization (b) for Li|Li(PEEIA-co-PEEPSI)/PVDF-HFP membrane|Li symmetric cell at room temperature, polarized with a potential of 100 mV.

Table S1. The measured parameters and the calculated t_{Li+} of the PVDF-HFP/PEEIA-co-LiPEEPSI membrane.

Electrolyte	$I_0(\mu A)$	$I_s(\mu A)$	$R_0(\Omega)$	$R_s(\Omega)$	t_{Li+}
Li(PEEIA-co-PEEPSI)	2.47	2.25	5.223	7.237	0.91

Reference

1 Y. Zhang, J. Ting, R. Rohan, W. Cai, J. Li, G. Xu, Z. Chen, A. Lin, H. Cheng, *J Mater Sci.* **2014**, *49*, 3442.

2 A. Ghosh , C. S. Wang, P. Kofinas, *J Electrochem Soc.*, **2010**, 157, A846-A849.